ME 7310 – Final Project
Incompressible Navier-Stokes Solver

Jonathan Sullivan
Mechanical and Industrial Engineering Department
Northeastern University

December 11, 2013

Abstract

In this project a two-dimensional (2D) incompressible laminar flow solver is developed for a lid-driven cavity flow. The governing Navier-Stokes and continuity equations are simplified using the vorticity-stream function formulation. A numerical algorithm is implemented using an explicit forward time second order central space (FTCS) finite difference discretization for the vorticity transport equation. The numerical algorithm also implements an explicit point Gauss-Seidel method with successive over-relaxation (PSOR) to solve for the stream function in order to obtain the x and y velocity components. The algorithm is run until a steady-state solution is found, which is evaluated based on a norm of the residual vector of the vorticity and a specified convergence criterion.

To verify the numerical results, a grid refinement study was conducted. Validation of the numerical solution was performed by comparing results for velocity, vorticity, and stream function with those obtained by Ghia *et al.* [1]

1 Problem Definition

In this project the 2D incompressible flow in a lid driven cavity is solved for a Reynolds number of 400 up until steady-state. The governing equations for the continuity and Navier-Stokes are:

$$\frac{\partial u}{\partial x}+\frac{\partial v}{\partial y}=0 \tag{1}$$

$$\frac{\partial u}{\partial t}+u\frac{\partial u}{\partial x}+v\frac{\partial u}{\partial y}=-\frac{1}{\rho}\frac{\partial p}{\partial x}+\nu\nabla^2 u \tag{2}$$

$$\frac{\partial v}{\partial t}+u\frac{\partial v}{\partial x}+v\frac{\partial v}{\partial y}=-\frac{1}{\rho}\frac{\partial p}{\partial y}+\nu\nabla^2 u \tag{3}$$

The difficulty in solving the three governing equations of the flow is due to the pressure term. A simplification of the equations can be made through the use of stream function and vorticity [2]. The stream function for the 2D flow, $\psi(x,y,t)$, is expressed in terms of the velocity components as:

$$u = \frac{\partial \psi}{\partial y}, \quad v = -\frac{\partial \psi}{\partial x} \tag{4}$$

Vorticity for the 2D flow in the x-y plane is expressed as:

$$\omega = \frac{\partial v}{\partial x} - \frac{\partial u}{\partial y} \tag{5}$$

The simplified system of equations [3] is composed of the vorticity transport equation (6) and the stream function equation (7).

$$\frac{\partial \omega}{\partial t} + u\frac{\partial \omega}{\partial x} + v\frac{\partial \omega}{\partial y} = \nu\left(\frac{\partial^2 \omega}{\partial x^2} + \frac{\partial^2 \omega}{\partial y^2}\right) \tag{6}$$

$$\frac{\partial^2 \psi}{\partial x^2} + \frac{\partial^2 \psi}{\partial y^2} = -\omega \tag{7}$$

The domain of interest is a square cavity with $0 \le x \le 1, 0 \le y \le 1$. The walls are stationary at $x = 0$, $x = 1$, and $y = 0$ (*i.e.* $u = v = 0$), while the wall at $y = 1$ moves along its plane with a velocity of $u = 1$, $v = 0$. It is assumed that there is a no-slip boundary condition at each wall. Since the problem is solved until steady-state, initial conditions for velocity, stream function, and vorticity are all assumed to be zero at internal nodes of the computational grid.

2 Numerical Solution Procedure

The first step in the numerical algorithm is to implement the boundary and initial conditions from the problem definition for velocity, vorticity, and stream function. The next step is to use the values of velocity, vorticity, and stream function at the initial time layer *n* to calculate the vorticity $\omega_{i,j}^{n+1}$ at interior nodes of the computational grid. The following explicit FTCS finite difference discretization of Equation (6) is implemented:

$$\begin{aligned}\frac{\omega_{i,j}^{n+1} - \omega_{i,j}^{n}}{\Delta t} = &-\frac{u_{i+1,j}^{n}\omega_{i+1,j}^{n} - u_{i-1,j}^{n}\omega_{i-1,j}^{n}}{2\Delta x} - \frac{v_{i,j+1}^{n}\omega_{i,j+1}^{n} - v_{i,j-1}^{n}\omega_{i,j-1}^{n}}{2\Delta y} \\ &+ \frac{1}{Re}\left[\frac{\omega_{i+1,j}^{n} - 2\omega_{i,j}^{n} + \omega_{i-1,j}^{n}}{(\Delta x^2)} + \frac{\omega_{i,j+1}^{n} - 2\omega_{i,j}^{n} + \omega_{i,j-1}^{n}}{(\Delta y^2)}\right]\end{aligned} \tag{8}$$

The finite difference scheme of Equation (8) has truncation error of the order of $O[(\Delta x)^2, (\Delta y)^2, (\Delta t)]$, and is consistent since $(\Delta x)^2 \to 0, (\Delta y)^2 \to 0, (\Delta t) \to 0$ as the step sizes are decreased, thus the truncation error vanishes. This scheme is subject to the following stability conditions:

$$\Delta t \leq \frac{1}{2/Re}\left[\frac{1}{(\Delta x)^2}+\frac{1}{(\Delta y)^2}\right]^{-1} \text{ and } \Delta t \leq \frac{2/Re}{\left(u_{i,j}^2+v_{i,j}^2\right)} \quad (9)$$

After vorticity is computed at the interior nodes, the next step is to compute the values for the stream function $\psi_{i,j}^{n+1}$ at the *n+1* time layer. This is accomplished through implementation of the following explicit point Gauss-Seidel method with successive over-relaxation (PSOR) formulation of the Poisson Equation (7):

$$\psi_{i,j}^{(k+1)} = (1-r)\psi_{i,j}^{(k)} + \frac{r}{2(1+\beta^2)}\left[\Delta x^2\omega_{i,j}^{(k)} + \psi_{i+1,j}^{(k)} + \psi_{i-1,j}^{(k+1)} + \beta^2\left(\psi_{i,j+1}^{(k)} + \psi_{i,j-1}^{(k+1)}\right)\right] \quad (10)$$

where *r* is the relaxation factor, $\beta = \frac{\Delta x}{\Delta y}$, the current iteration layer is (*k*), and the next iteration layer is (*k+1*). The finite difference scheme of Equation (10) has truncation error of the order of $O[(\Delta x)^2, (\Delta y)^2]$, and is consistent since as $(\Delta x)^2 \to 0, (\Delta y)^2 \to 0$ with decreasing grid size, the truncation error vanishes. The following norm of the residual vector of the stream function is used to determine convergence of the iterative process:

$$R^{(k)} = \left\|\psi^{(k+1)}(i,j) - \psi^{(k)}(i,j)\right\| / \left\|\psi^{(k)}(i,j)\right\| \quad (11)$$

The convergence criterion implemented for the PSOR method is 10^{-5}. Once the values for stream function are computed, the velocity components $u_{i,j}^{n+1}$ and $v_{i,j}^{n+1}$ for internal nodes can be computed using the second order central difference approximations from Equations (12) and (13), respectively.

$$u_{i,j}^{n+1} = \frac{\psi_{i,j+1}^{n+1} - \psi_{i,j-1}^{n+1}}{2\Delta y} \quad (12)$$

$$v_{i,j}^{n+1} = -\frac{\psi_{i+1,j}^{n+1} - \psi_{i-1,j}^{n+1}}{2\Delta x} \quad (13)$$

The Neumann boundary conditions for vorticity can now be evaluated using forward difference approximations at the top and left walls, and backwards difference approximations at the right and bottom walls. For the sake of simplicity, first order finite-difference approximations were used to compute the values of vorticity at the boundaries. Although this is of lower order accuracy than the FTCS and PSOR schemes, sufficient grid refinement was implemented to increase the accuracy of the solution for vorticity at the boundaries. The final step is to evaluate the norm of the residual vector of the vorticity:

$$R^{(k)} = \left\|\psi^{(k+1)}(i,j) - \psi^{(k)}(i,j)\right\| / \left\|\psi^{(k)}(i,j)\right\| \quad (14)$$

If the norm from Equation (14) is less than 10^{-5} the solution has converged. If the solution has not converged, the numerical algorithm is repeated until the convergence criterion is satisfied, which indicates the steady-state solution.

3 Numerical Results

In order to verify the solution, a grid independent study was performed by implementing the following three different refinement levels of equally spaced grids: 21 x 21 nodes, 41 x 41 nodes, and 81 x 81 nodes. Results for *u* and *v* velocity components are displayed in Figure 3-1 and Figure 3-2, respectively. Results from Ghia [1] are also plotted for purposes of validation.

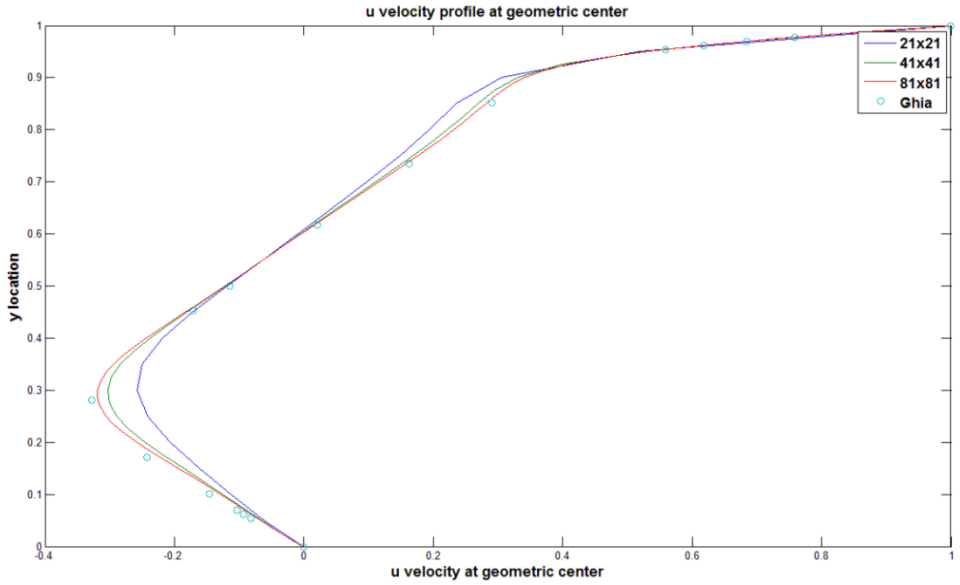

Figure 3-1: u velocity profile at geometric center

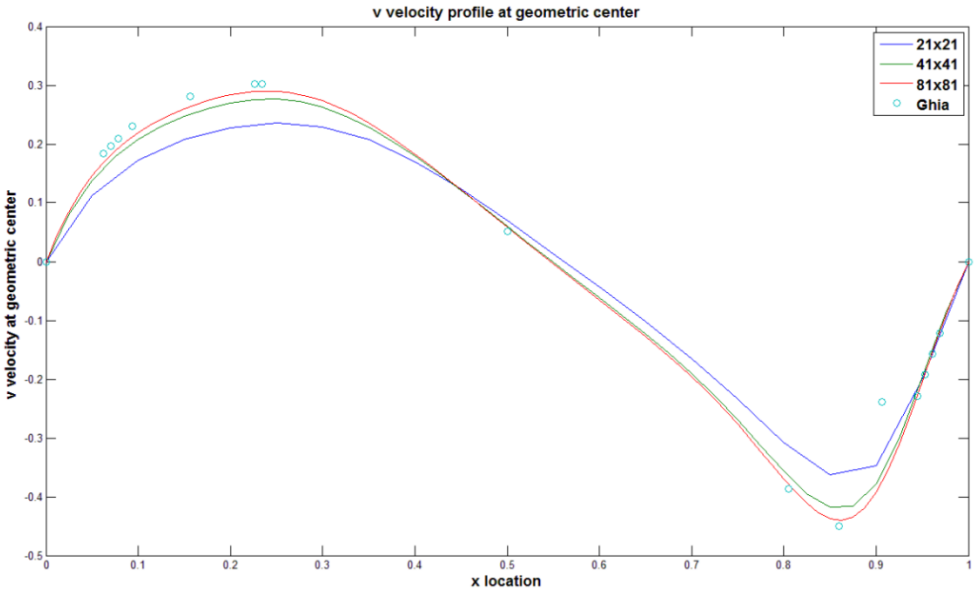

Figure 3-2: v velocity profile at geometric center

As the grid is refined to 81x81 nodes, the numerical results for *u* and *v* undoubtedly show that the solution is converging. The numerical solutions computed are also approaching the results obtained by Ghia [1], which were computed on a 129x129 node grid. Based on the results obtained, it can be said that the numerical solutions computed have been verified and validated.

It should be noted that even with the implementation of the relaxation factor, the CPU time for computations on the 81x81 node grid is about twelve minutes. At the expense of increased accuracy, and in order to keep the computational time relatively low, it was deemed that further refinement beyond 81x81 nodes was unnecessary.

Another method of validation was to compare contour plots of stream function and vorticity obtained by the numerical algorithm with those shown in the literature. Contour plots of stream function and vorticity obtained by the numerical algorithm are shown in Figures 3-3 and 3-4 respectively.

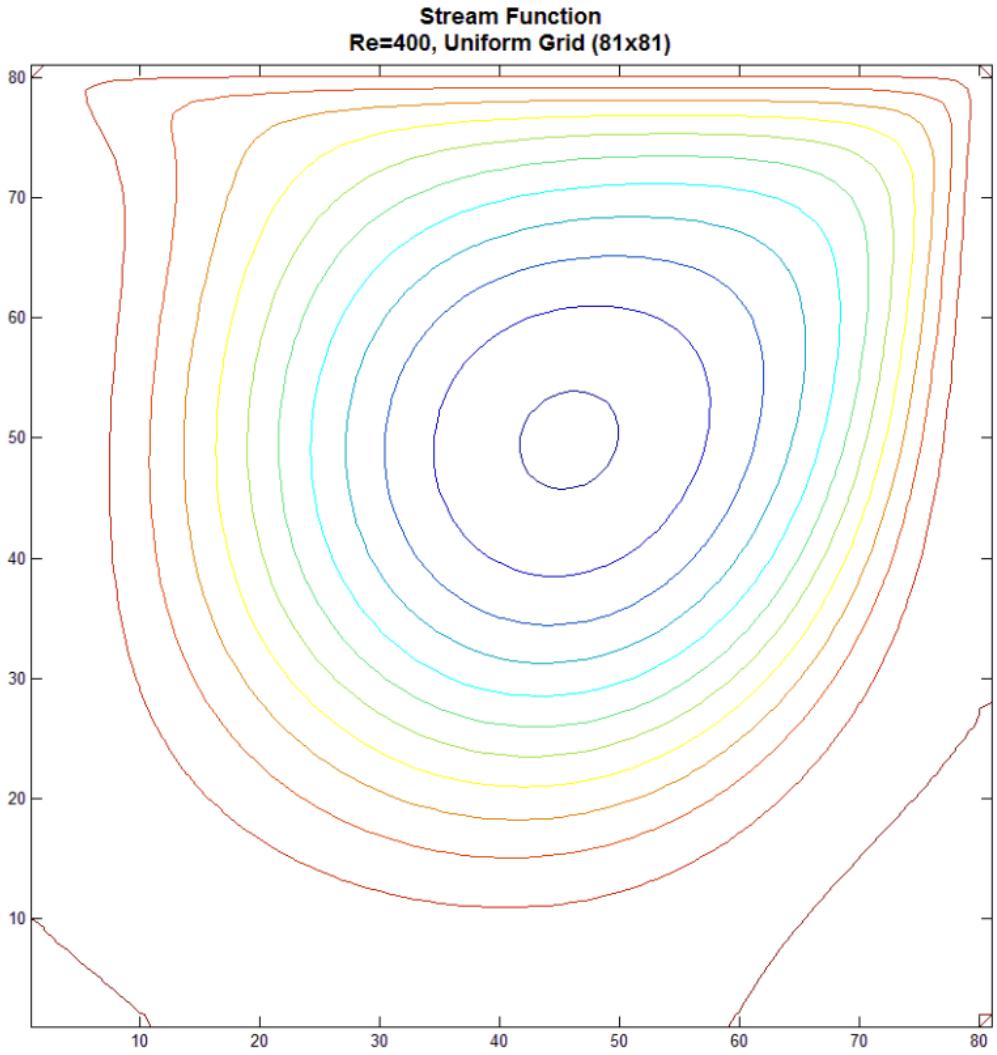

Figure 3-3: Contour plot of stream function

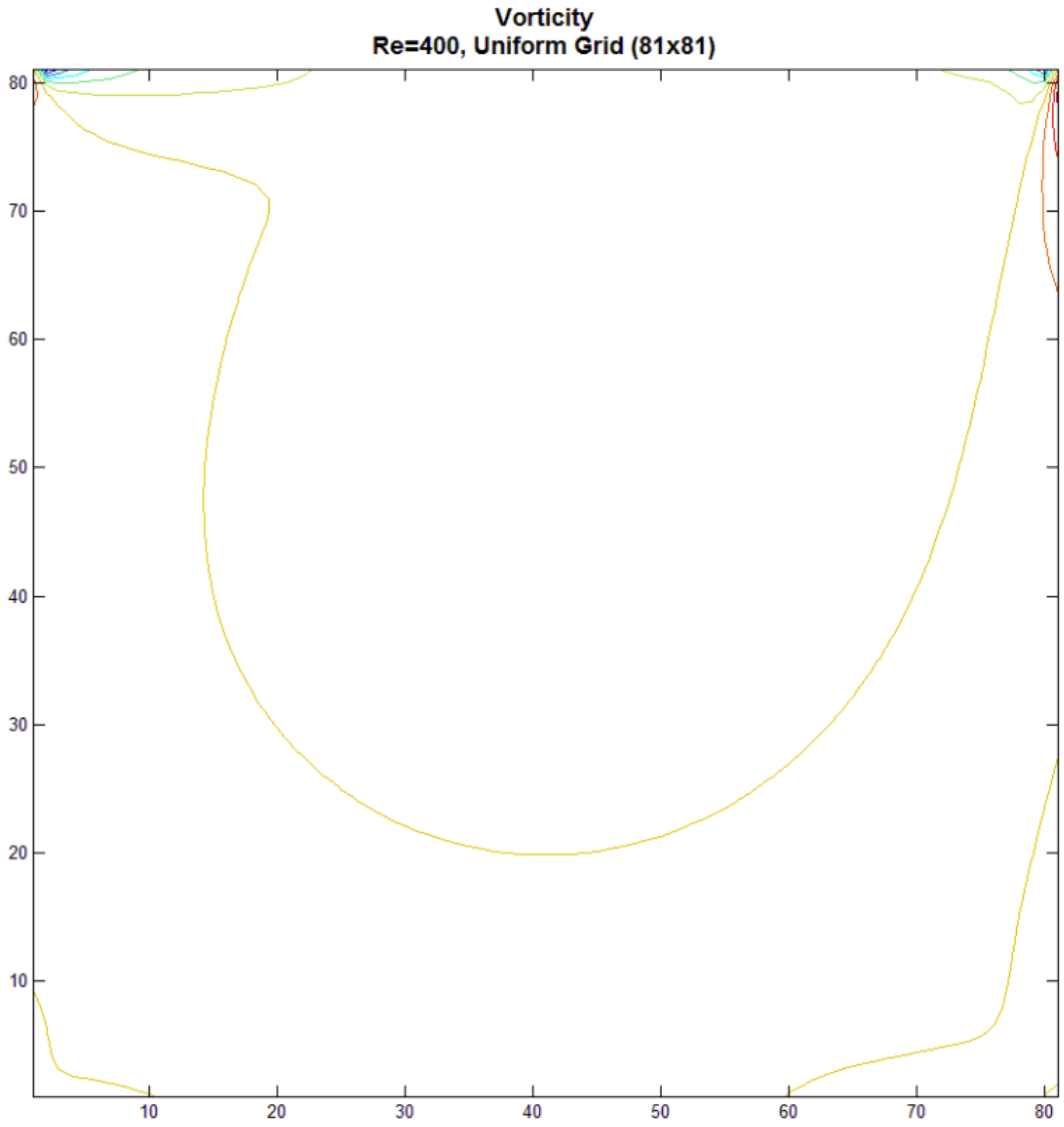

Figure 3-4: Contour plot of vorticity

The contour plot of stream function (Figure 3-3) clearly shows the streamline pattern for the primary vortex, while additional vortices seem to be forming at the bottom corners of the cavity. The results appear to compare relatively well with those obtained in Figure 3 of the literature for a Reynolds number of 400, although the results obtained in the literature were computed on a finer grid (129x129). Due to the computational cost, a solution was not computed on a grid resolution finer than 81x81. Increasing the resolution may assist in representing the vortices forming at the bottom corners of the cavity, which are visible in Figure 3 of the literature.

The contour plot of vorticity (Figure 3-4) is also in good agreement with results obtained in the literature (Figure 4). As was the case with stream function, a grid of 81x81 nodes was used to compute the solution for a Reynolds number of 400. Again, refining the grid further may help in capturing the vorticity contours to more close match the results obtained in the literature on a 129x129 node grid.

The final method of validation was to compare the results computed for vorticity along the moving boundary with those obtained in the literature. Results of the absolute value of vorticity are compared in Figure 3-5.

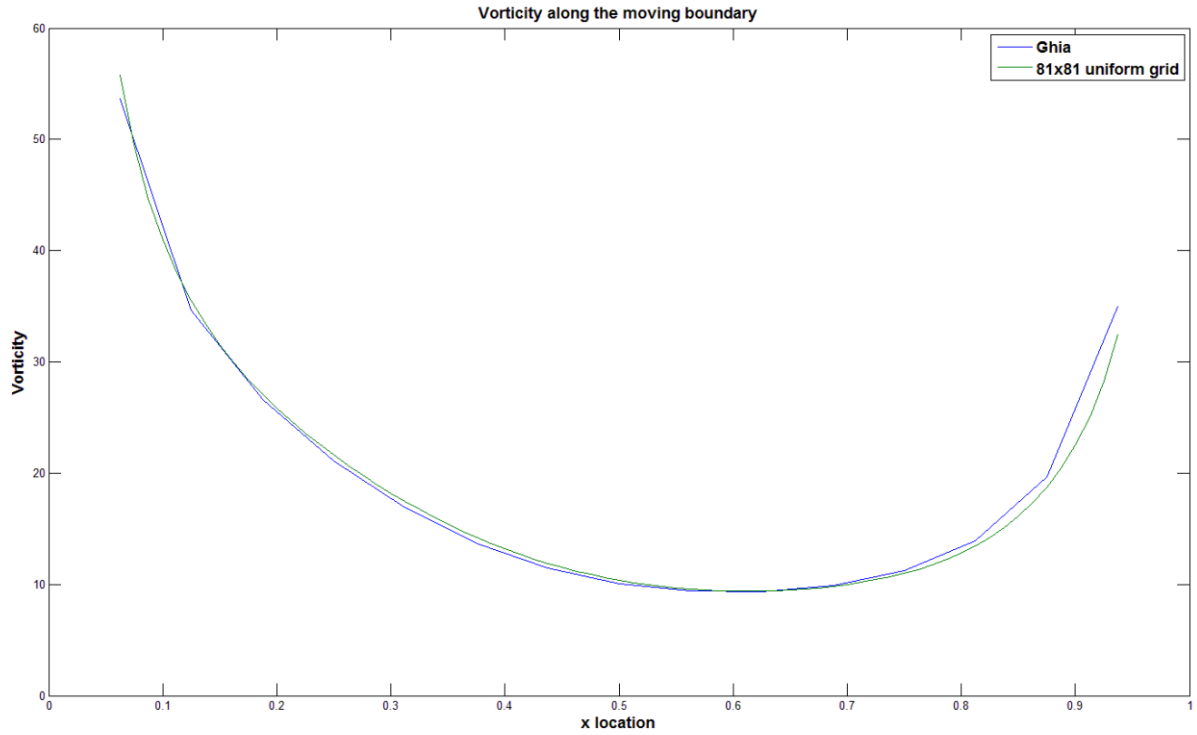

Figure 3-5: Vorticity along the moving boundary

Results of vorticity along the moving boundary computed using the numerical algorithm are in good agreement with results obtained from the literature. Implementing a finer grid and higher order accuracy boundary conditions for vorticity would increase the accuracy of the solution, but the computational cost would increase.

4 References

[1] U. Ghia, K.N. Ghia, and C.T. Shin, "High-Re Solutions for Incompressible Flow Using the Navier-Stokes Equations and a Multigrid Method," *Journal of Computational Physics* 48, 387-411 (1982).

[2] Essential Computational Fluid Dynamics, by O. Zikanov, John Wiley & Sons, Inc., 2010

[3] Computational Fluid Dynamics, by K.A. Hoffman.